Short Communication

Synthetic cannabinoid quinones: preparation, in vitro antiproliferative effects and in vivo prostate antitumor activity

Paula Morales[a], Diana Vara[b], María Goméz-Cañas[c], María C. Zúñiga[d], Claudio Olea-Azar[d], Pilar Goya[a], Javier Fernández-Ruiz[c], Inés Díaz-Laviada[b]*, Nadine Jagerovic[a]*

[a]Instituto de Química Médica, CSIC, Calle Juan de la Cierva, 3, 28006 Madrid, Spain

[b]Departamento de Bioquímica y Biología Molecular, Facultad de Medicina, Universidad de Alcalá, Alcalá de Henares, 28871 Madrid, Spain

[c]Departamento de Bioquímica y Biología Molecular, Facultad de Medicina, CIBERNED, IRYCIS, Universidad Complutense de Madrid, 28040 Madrid, Spain

[d]Departamento de Química Inorgánica y Analítica, Facultad de Ciencias Químicas y Farmacéuticas, Universidad de Chile, Casilla 233, Santiago 1, Chile

*Corresponding authors. Tel.: 34-91-562-2900; fax: 34-91-564-4853; *E-mail address*: nadine@iqm.csic.es (N. Jagerovic); Tel: 34-91-885-5141; Fax: 34-91-885-4585; *E-mail address*: ines.diazlaviada@uah.es (I. Díaz-Laviada)

***Abbreviations*:** LNCaP, lymph node carcinoma prostate; PC-3, prostate cancer; HepG2, heptoblastoma; HT-29, human colon adenocarcinoma; ROS, reactive oxygen specie; EBNA, Epstein-Barr virus nuclear antigen; TBAP, tetrabuthylammonium perchlorate; PBS, phosphate buffered saline; S.D., standard deviation; S.E., standard error; FITC, fluorescein isothiocyanate; PI, propidium iodide.

Keywords: Cannabinoid; quinone; prostate cancer; antitumor; chromenopyrazoledione; antiproliferative; electrochemistry.

HIGHLIGHTS

> Anticancer activity involving quinone and cannabinoid antitumor properties.

> Compound **4** causes G0/G1 phase arrest and apoptosis on LNCaP prostate cancer cells.

> Antiproliferative action of **4** is mediated by oxidative stress and CB_1 receptor.

> Compound **4** (2mg /Kg) blocks the growth of hormone-sensitive prostate cancer in vivo.

ABSTRACT

Chromenopyrazolediones have been designed and synthesized as anticancer agents using the multi-biological target concept that involves quinone cytotoxicity and cannabinoid antitumor properties. In cell cytotoxicity assays, these chromenopyrazolediones have antiproliferative activity against human prostate cancer and hepatocellular carcinoma. It has been shown that the most potent, derivative **4** (PM49), inhibits prostate LNCaP cell viability (IC_{50} = 15 µM) through a mechanism involving oxidative stress, PPARγ receptor and partially CB_1 receptor. It acts on prostate cell growth by causing G_0/G_1 phase arrest and triggering apoptosis as assessed by flow cytometry measurements. In the in vivo treatment, compound **4** at 2 mg/Kg, blocks the growth of LNCaP tumors and reduces the growth of PC-3 tumors generated in mice. These studies suggest that **4** is a good potential anticancer agent against hormone-sensitive prostate cancer.

1. Introduction

Prostate cancer is the second most common cancer worldwide for males. The rates have increased in recent years as its detection has improved in the younger men and as life expectancy is longer [1]. Therefore, there are extensive, ongoing efforts to develop new therapeutic strategies to treat prostate cancer [2].

A large diversity of biological signaling-pathways is implicated in the pathogenesis of cancer. Appropriate treatment of neoplasms often depends on pharmaceutical intervention at multiple pathways, with a combination of different drugs. In this context, targeting different anticancer modes of action in a single molecule is a significant challenge [3, 4]. Our interest in cannabinoid ligands and antiproliferative agents has led to the development of molecules which includes in one entity cannabinoid and quinone features.

In the last decade, cannabinoids (Sativex® and Marinol®) have been clinically used as palliative treatment in chemotherapy [5]. They reduce emesis, stimulate appetite and relieve pain. More recently, increasing biochemical and pharmacological data have showed that cannabinoids can modulate tumor growth, apoptosis and angiogenesis in various types of cancer [6-13]. ENREF_3 Evidences have been recently reported on the deregulation of the endocannabinoid system in prostate tumor [14]. Thus, this system provides a new therapeutic target for this type of cancer. Interestingly, its modulation by endocannabinoid hydrolysis inhibitors produces antiproliferation of prostate carcinoma [15, 16].

On the other hand, the well-established antitumor properties of quinones are still the focus of much research. Nowadays cytotoxic quinones represent an important group of antineoplastic drugs [17]. They are mainly involved in oxidative phosphorylation and

electron transport processes. Therefore, their cytotoxicity activity can be accounted for by their bioreductive and/or Michael acceptor properties that produce oxidative stress.

Few years ago, Kogan *et al* reported the antiproliferative activity of three quinone derivatives of phytocannabinoid (Fig. 1: HU-331, HU-336, HU-345) [18]. The most effective, HU-331, reduced growth of human colon carcinoma HT-29 cells in nude mice. Its antiproliferative effect was not attributed to a mechanism involving cannabinoid receptors since it does not have any affinity for these receptors [19]. Accordingly, developing new antitumoral agents with dual mechanism, cannabinoid and oxidative stress, is highly valued to improve the efficacy and overcome side-effects related to quinones.

Recently, we published the cannabinoid properties of a new family of chromenopyrazoles [20], fully selective CB_1 receptor ligand lacking psychoactive effects. Following with chromenopyrazole as scaffold we report herein the synthesis of the corresponding quinone related derivatives (**4**-**6**). Their ability to bind to CB_1 and CB_2 cannabinoid receptors, to generate reactive oxygen species, and to produce antiproliferative properties in vitro and in vivo will be discussed. Thus, we report the first antitumoral quinone which antiproliferative activity proceeds through various mechanisms including cannabinoid receptors.

2. Results

2.1. Chemistry and electrochemistry

The starting 7-(1',1'-dimethylheptyl)-dihydro-4,4-dimethylchromeno[4,3-c]pyrazol-9-ols **1**-**3** were prepared according to a synthetic procedure previously reported by us [20]. Scheme 1 outlines the synthesis of the cannabinoid quinones **4**-**6**. The reagent [bis(trifluoro-acetoxy)iodo]benzene $[(CF_3CO_2)_2IC_6H_5]$ (BTIB) was used to oxidize the chromenopyrazoles

1-**3** to the corresponding quinones **4**-**6**. This oxidative reagent is a hypervalent iodine compound that allows regio-controlled oxidations of phenol to *para*-quinones under mild conditions [21, 22]. The 7-(1',1'-dimethylheptyl)-dihydro-4,4-dimethylchromeno[4,3-*c*]pyrazol-6,9-diones **4-6** were obtained in moderate yields (21-36%).

Since most of the biological functions of quinones are associated with their redox activity, the electrochemical properties of 7-(1',1'-dimethylheptyl)-1,4-dihydro-4,4-dimethylchromen[4,3-c]pyrazol-6,9-dione (**4**; PM49) and 7-(1',1'-dimethylheptyl)-2-ethyl-2,4-dihydro-4,4-dimethylchromen[4,3-c]pyrazol-6,9-dione (**6**) have been studied by cyclic voltammetry. Chromenopyrazoledione **5** is structurally close enough to derivative **6** to consider that both compounds show similar electrochemical behavior. Chromenopyrazolediones **4** and **6** displayed comparable voltammetric behavior, showing two well-defined reduction waves in DMSO. The first wave for both quinones studied corresponded to a cuasi-reversible one-electron transfer. The reverse scan showed the anodic counterpart of the reduction waves (Fig. 2). According to the standard reversibility criteria, this couple corresponds to a cuasi-reversible diffusion-controlled one-electron transfer. It is attributable to the reduction of quinone to semiquinone that involves a stable anion radical at room temperature. The second couple is irreversible over the whole range of sweep rates used (0.1 at 2.0 V/s). We can attribute this wave to the production of a hydroquinone derivative.

Electron spin resonance (ESR) experiments were carried out in order to correlate the cytotoxicity to the formation of radicals. The semiquinone free radicals were prepared in situ by electrochemical reductions in DMSO, applying a potential corresponding to the first wave for **4** or **6** obtained from the cyclic voltammetric experiments. The interpretation of the ESR spectra by means of a simulation process has led to the determination of the coupling constants for all the magnetic nuclei, confirmed by theoretical calculations. The ESR

spectrum of **4** was analyzed and simulated in terms of one doublet from hydrogen nuclei of the quinone moiety; the hyperfine constant was 2.635 gauss. Fig. 3 shows the ESR experimental and simulation spectra. Similar hyperfine pattern was found for **6** with hydrogen hyperfine constant value of 2.925 gauss.

The results obtained with these electrochemical experiments showed that the redox potentials of **4** and **6** are low enough to generate reactive oxygen species (ROS). Therefore, these quinone radical entities should be able to produce oxidative stress.

2.2. Biology

2.2.1. Cannabinoid receptor affinity

The binding affinity of the chromenopyrazolediones **4**-**6** was assessed through radioligand competition binding experiments. The ability of **4**-**6** to displace [^{3}H]CP55940 from human cannabinoid CB_1 or CB_2 receptors transfected into HEK293 EBNA cells was evaluated. Standard cannabinoid ligand WIN55,212-2 was also tested for comparison with the new compounds. The experimental binding affinities of **4**-**6** and WIN55,212-2 are reported in Table 1. Interestingly, **4** showed significant affinity in the nanomolar (submicromolar) range both CB_1 and CB_2 receptors. This is a noteworthy feature since the only cannabinoid quinones reported so far did not show affinity for the cannabinoid receptors, as already mentioned [18].

2.2.2. In vitro antiproliferative effect on cancer cells

The antiproliferative effect of chromenopyrazolediones **4**-**6** was evaluated against the cancer cell lines HepG2, LNCaP and PC-3. HepG2 is a hepatocellular carcinoma-derived cell line, LNCaP is an androgen-dependent prostate cancer-derived cell line and PC-3 is an androgen-refractory prostate cancer-derived cell line. Different doses of **4**-**6** were added to cell cultures

for 48h and cell viability was assayed by colorimetric measurements using 3-(4,5-dimethylthiazol-2-yl)-2,5-diphenyltetrazolium bromide (MTT) as a dye. As showed in Fig. 4, **4**-**6** were more effective in prostate than in hepatocellular carcinoma cells, being **4** the most potent with an IC_{50} of 30 µM for HepG2 cells and 15 µM for prostate cancer LNCaP and PC-3 cells. Therefore, the chromenopyrazoledione **4** (PM49) was selected for following investigations in prostate cancer cells.

2.2.3. Mechanism of antiproliferative action

To study the effect of the chromenopyrazoledione **4** on the cell cycle of prostate cells, flow cytometry analysis were carried out. Results shown in Fig. 5 demonstrate that **4** increased the amount of cells in the sub G_0/G_1 phase of the cell cycle. This result suggests that compound **4** induces growth arrest and cell death.

For quantifying the percentage of apoptotic cells after drug treatment, LNCaP and PC-3 cells were stained with Annexin V-FITC/PI. Results show that the rate of late apoptotic cells (see Fig. 6: Annexin V-FITC positive/PI positive, upper right quadrant) in **4**-treated cells was statistically increased compared to the control cells. Early apoptotic cells (Annexin V-FITC positive/PI negative) were nearly 6 % in LNCaP cells and nearly 4% in PC-3 cells. These findings indicate that compound **4** induces a significant percentage of apoptosis in prostate cancer cells being more efficient in promoting apoptosis in the androgen-sensitive LNCaP cell line.

In order to further study the underlying mechanism of cannabinoid quinone **4**-induced prostate cell death, the IC_{50} dose of each compound was tested against LNCaP cells in the presence of the CB_1 antagonist SR141716 (SR1, also named rimonabant), the CB_2 antagonist SR144528 (SR2), the antioxidant *N*-acetylcysteine (NAC), or the peroxisome proliferator-activated receptor gamma (PPARγ) antagonist GW 9662. LNCaP cells were incubated for

48h with **4** along with SR1, SR2, NAC, or GW 9662. Then, cell viability was assayed by MTT. The CB_1 antagonist (SR1) as well as the PPARγ antagonist (GW 9662) [23], and the antioxidant (NAC) were able to significantly reduce the inhibition of cell viability induced by **4** (Fig. 7). These results indicate that the chromenopyrazoledione **4** inhibits cell viability through a mechanism involving oxidative stress, PPARγ receptors and partially CB_1 receptors. It is noteworthy that only SR1 and not SR2 prevent the antiproliferative effect of **4** in LNCaP cells albeit **4** exhibiting higher affinity for CB_2 than for CB_1. This might be explained by a low expression of CB_2 receptors in LNCaP cells that has already been observed in previous reports [24]. The antioxidant NAC did not only prevent **4**-induced cell death but even slightly increased cell viability.

2.2.4. In vivo antitumor activity

To investigate the ability of compound **4** to inhibit prostate tumor growth in vivo, tumor xenografts by subcutaneous inoculation of LNCaP or PC-3 cells in nude mice were generated. Mice were daily treated with vehicle (control), or 2 mg/kg of **4** intraperitoneally administered for 15 days. As shown in Fig. 8, treatment with **4** almost totally blocked the growth of LNCaP tumors whereas it inhibited the growth of PC-3 tumors by 40 %. The final tumor volume was smaller in all **4**-treated mice.

2.3. ADME parameters *in silico*

Absorption, distribution, metabolism, and excretion (ADME) of preclinical drug candidate are of interest in the early screening phase of drug development. Some of the relevant ADME properties of **4** were calculated on the conformer of global minimum energy. The predicted data indicated that Lipinski and Jorgensen pharmacokinetics rules are followed. The prediction of solubility, blood-brain barrier permeability, human oral absorption, potassium

channel characteristic of long QT syndrome suggests favorable druggability profile of **4** (Table 2).

3. Discussion and Conclusion

Chromenopyrazolediones **4**-**6** exert antiproliferative effects on the cancer cells HepG2, LNCaP and PC-3. They are more efficient and potent against prostate cancer than against hepatocellular carcinoma. Flow cytometry assessments demonstrate that **4** (PM49) inhibits prostate cancer cell growth by causing G_0/G_1 phase arrest and triggering apoptosis. Comparison of the antitumor activity of **4** in the two prostate cancers LNCaP and PC-3 indicates that **4** is more efficient in androgen-sensitive prostate cancer cells (LNCaP), which must be considered a significant finding. The cornerstone of medical treatment for advanced prostate cancer has been hormonal therapy, intended to lower testosterone levels, known as Androgen Deprivation Therapy (ADT) although the reduction of clinical symptoms and tumor growth is accompanied by systemic consequences of testosterone deficiency including hot flashes, weight gain, gynecomastia, osteoporosis, anemia and insulin resistance [25, 26]. Androgen deprivation is associated with a gradual transition of prostate cancer cells through a spectrum of androgen dependence, androgen sensitivity, and ultimately androgen independence. Too often the appearance of hormone refractory cancer cells eventually leads to the recurrence of cancer which turns to a hormone-independent state, also called castration-recurrent prostate cancer (CRPC) which has a more aggressive phenotype and is unresponsive to further hormonal therapy whereby prognosis is very poor. Therefore, to find a treatment which could totally block the first androgen-dependent prostate cancer stages would be a very good challenge to move forward and in this sense the results obtained with **4** offers an excellent opportunity.

An important aspect of this study is that compound **4** exhibits moderate affinity, in the high nanomolar range, for cannabinoid receptors CB_1 and CB_2 with a 2-3 fold greater preference for CB_2. Interestingly, we have shown that part of its antiproliferative activity was mediated by the CB_1 cannabinoid receptor, as it was partly sensitive to blockade with the CB_1 receptor antagonist SR1. By contrast, the CB_2 receptor antagonist SR2 was not effective indicating that CB_2 receptors are not involved, which is in agreement with the fact that this type of receptors have a low expression in LNCaP tumor cells [24]. Other mechanisms besides the binding to the cannabinoid receptor may be operating in its antiproliferative effect of compound **4**. For example, we have found that the PPARγ receptor antagonist significantly prevents the cytotoxic effect of **4**. The fact that PPARγ receptors may be involved in the mechanism of action of **4** is not that surprising since a potent activation capacity of PPARγ by other quinone derivatives with anticancer activity has already been reported [27, 29]. ENREF_7 The possible participation of PPARγ receptor in the underlying mechanism of compound **4** antiproliferative effects is a new finding that will be explored in future research.

The redox properties of **4** evaluated by cyclic voltammetry and electron spin resonance show that the redox potentials are low enough to generate reactive oxygen species (ROS). Therefore, these quinone radical entities should be able to produce oxidative stress. In fact, the antioxidant NAC significantly reduces the antiproliferative effect of **4** supporting the hypothesis that oxidative stress contributes to the cytotoxicity of **4**.

Chromenopyrazoledione **4** exerts an effective prostate tumor activity in vivo at a dose of 2mg/Kg. The tumor size in treated mice decreased significantly for androgen-refractory prostate cancer (PC-3). In the case of the androgen-dependent prostate cancer (LNCaP), the treatment with **4** totally inhibited the growth of the tumor compared with the control.

The concentrations of **4** used in this study are quite similar to those employed by other authors who have explored antitumor activity of other quinones on PC-3 cells [30-32]. Likewise, concentrations used in our in vivo study are similar to those used with cannabidiol derived quinone [19] and far from the doses capable to produce toxicity [33]. Therefore, **4** may be relevant for preclinical studies. Moreover, the predicted ADME properties suggest favorable druggability profile.

Taken together, the data provide evidence supporting that the chromenopyrazoledione **4** discovered in this study is a potential anticancer agent against hormone-sensitive prostate cancer and has a high potential to be considered for development into a new anticancer drug.

4. Experimental Section

4.1. Chemistry

4.1.1. General methods and materials

All commercially available reagents and solvents were used without further purification. Column chromatography was performed using silica gel 60 (230-400 mesh). The purity of final compounds as determined by HPLC/MS is > 95%. Analytical HPLC/MS analysis was performed on a Waters 2695 HPLC system equipped with a Photodiode Array 2996 coupled to Micromass ZQ 2000 mass spectrometer (ESI-MS), using a reverse-phase column SunFire^{TM} (C-18, 4.6 x 50 mm, 3.5 μm) and 5 min gradient A: MeCN/0.08% formic acid, B: H_2O/ 1% formic acid visualizing at λ = 254 nm. Elemental analyses of all synthesized compounds were performed using a LECO CHNS-932 apparatus. Analyses indicated by the symbols of the elements or functions were within ± 0.4 % of the theoretical values. ^{1}H and ^{13}C NMR spectra were recorded on a Bruker 300 (300 and 75 MHz) at 25ºC. Samples were prepared as solutions in deuterated solvent and referenced to internal non-deuterated solvent peak. Chemical shifts were expressed in ppm (δ) downfield of tetramethylsilane. Melting

points were determined on a MP70 Mettler Toledo apparatus. Chromenopyrazoles **1**-**3** were prepared according to procedures previously published by us [20].

4.1.2. Preparation of compounds

4.1.2.1. 7-(1',1'-Dimethylheptyl)-1,4-dihydro-4,4-dimethylchromeno[4,3-c]pyrazol-6,9-dione (**4**)

To a solution of 7-(1',1'-dimethylheptyl)-1,4-dihydro-4,4-dimethylchromeno[4,3-*c*]pyrazol-9-ol (**1**) [20] (130 mg, 0.38 mmol) in MeCN/ H_2O (6:1, 2.5 mL) a solution of BTIB (490 mg, 1.14 mmol) in 2 mL of MeCN/ H_2O (6:1) was added dropwise. The reaction mixture was stirred at room temperature for 15 min, neutralized with aqueous $NaHCO_3$ satured solution, and extracted with diethyl ether. The organic layer was washed with H_2O, dried over $MgSO_4$ and concentrated. Column chromatography on silica gel (hexanes/EtOAc 1:2) afforded the title compound as a red solid (29 mg, 21% yield); mp: 85.7 ºC; ^{1}H-NMR ($CDCl_3$) δ: 8.41 (bs, 1H, NH), 7.40 (s, 1H, 3-H), 6.69 (s, 1H, 8-H), 1.59 (bs, 6H, $OC(CH_3)_2$), 1.55-1.48 (m, 2H, 2´-H), 1.30 (s, 6H, $C(CH_3)_2$), 1.27-1.23 (m, 6H, 3´-H, 4´-H and 5´-H), 1.19 (bs, 2H, 6´H), 0.86-0.82 ppm (m, 3H, 7´-H); ^{13}C-NMR ($CDCl_3$) δ: 184.1 (6-C), 180.9 (9-C), 160.2 (5a-C), 161.2 (7-C), 137.8 (9b-C), 132.0 (8-C), 130.4 (9a-C), 129.5 (3-C), 113.8 (3a-C), 78.6 ($OC(CH_3)_2$), 43.3 (2´-C), 30.9 (1´-C), 29.6, 28.7 y 27.4 (3´-C, 4´-C and 5´-C); 25.1 ($C(CH_3)_2$), 23.2 ($OC(CH_3)_2$), 21.8 (6´-C), 14.0 ppm (7´-C); HPLC/MS: [A, 70% →100%], t_R: 3.37 min (98%), MS (ES^+, m/z) 357 $[M+H]^+$; Anal. C21H28N2O3 (C, H, N, O).

4.1.2.2. 7-(1',1'-Dimethylheptyl)-2,4-dihydro-2,4,4-trimethylchromeno[4,3-c]pyrazol-6,9-dione (**5**)

Prepared from 7-(1',1'-dimethylheptyl)-2,4-dihydro-2,4,4-trimethylchromeno[4,3-*c*]pyrazol-9-ol (**2**) [20] (35 mg, 0.1 mmol) and BTIB (129 mg, 0.3 mmol) by following the

procedure described for **4**. Column chromatography on silica gel (hexanes/EtOAc 1:4) afforded **5** as a red solid (12 mg, 33 % yield); mp: 89.7 ºC; ^{1}H- NMR ($CDCl_3$) δ: 7.36 (s, 1H, 3-H), 6.61 (s, 1H, 8-H), 3.95 (s, 3H, NCH_3), 1.84 (s, 6H, $OC(CH_3)_2$), 1.70 (bs, 2H, 2´-H), 1.33 (s, 6H, $C(CH_3)_2$), 1.26 (bs, 6H, 3´-H, 4´-H and 5´-H), 1.16-1.13 (m, 2H, 6´H), 0.85 ppm (t, *J* = 6,9 Hz, 3H, 7´-H); ^{13}C- NMR ($CDCl_3$) δ: 186.2 (6-C), 181.4 (9-C), 160.2 (5a-C), 155.0 (7-C), 139.6 (9b-C), 135.4 (8-C), 129.3 (9a-C), 126.9 (3-C), 115.7 (3a-C), 81.5 ($OC(CH_3)_2$), 43.0 (NCH_3), 40.9 (2´-C), 31.7 (1´-C), 30.8, 29.3 and 28.1 (3´-C, 4´-C and 5´-C), 27.5 ($C(CH_3)_2$), 23.4 ($OC(CH_3)_2$), 22.9 (6´-C), 14.6 ppm (7´-C); HPLC/MS: [A, 80% →100%], t_R: 2.43 min (100%), MS (ES^+, m/z) 371 $[M+H]^+$; Anal. $C_{22}H_{30}N_2O_3$ (C, H, N, O).

4.1.2.3. 7-(1',1'-Dimethylheptyl)-2-ethyl-2,4-dihydro-4,4-dimethylchromeno[4,3-c]pyrazol-6,9-dione (**6**)

Prepared from 7-(1',1'-dimethylheptyl)-2-ethyl-2,4-dihydro-4,4-dimethylchromeno[4,3-*c*]pyrazol-9-ol (**3**) [20] (61 mg, 0.16 mmol) and BTIB (212 mg, 0.49 mmol) by following the procedure described for **4**. Column chromatography on silica gel (hexanes/EtOAc 2:3) afforded **6** as a red solid (22 mg, 36 % yield); mp: 83.9 ºC; ^{1}H- NMR ($CDCl_3$) δ: 7.15 (s, 1H, 3-H), 6.50 (s, 1H, 8-H), 4.28 (q, *J* = 7.4 Hz, 2H, NCH_2CH_3), 1.72 (s, 6H, $OC(CH_3)_2$), 1.61-1.58 (m, 2H, 2´-H), 1.49 (t, *J* = 7.4 Hz, 3H, NCH_2CH_3), 1.30 (s, 6H, $C(CH_3)_2$), 1.23-1.10 (m, 8H, 3´-H, 4´-H, 5´-H and 6´-H), 0.89 ppm (t, *J* = 6.9 Hz, 3H, 7´-H); ^{13}C- NMR ($CDCl_3$) δ: 183.4 (6-C), 180.5 (9-C), 152.4 (5a-C), 151.4 (7-C), 137.2 (9b-C), 133.1 (8-C), 122.1 (3-C), 120.9 (3a-C), 110.6 (9a-C), 79.9 ($OC(CH_3)_2$), 46.6 (NCH_2CH_3), 39.7 (2´-C), 37.6 (1´-C), 31.6, 29.7 and 28.7 (3´-C, 4´-C and 5´-C), 26.6 ($OC(CH_3)_2$), 24.1 ($C(CH_3)_2$), 21.5 (6´-C), 14.6 (NCH_2CH_3), 13.0 ppm (7´-C); HPLC/MS: [A, 70% →100%], t_R: 3.86 min (96%), MS (ES^+, m/z) 385 $[M+H]^+$; Anal. $C_{23}H_{32}N_2O_3$ (C, H, N, O).

4.2. Electrochemistry

4.2.1. Cyclic voltammetry

DMSO (spectroscopy grade) was obtained from Aldrich. Tetrabuthylammonium perchlorate (TBAP), used as supporting electrolyte, was obtained from Fluka. Cyclic voltammetry was carried out using a Metrohm 693 VA instrument with a 694 VA Stand convertor and a 693 VA Processor, in DMSO (ca. 1.0×10−3 mol L−1), under a nitrogen atmosphere at room temperature, with TBAP (ca. 0.1 mol L−1), using a three-electrode cell. A mercury-dropping electrode was used as the working electrode, a platinum wire as the auxiliary electrode, and saturated calomel as the reference electrode.

4.2.2. ESR spectroscopy

ESR spectra were recorded in the X band (9.7 GHz) using a Bruker ECS 106 spectrometer with a rectangular cavity and 50 kHz field modulation. The nitro radicals were generated by electrolytic reduction in situ under the same conditions of temperature, atmosphere and concentrations stated at the voltammetric experiment. Simulations of the spectra were made using the Simfonia Version 1.25 software. The hyperfine splitting constants were estimated to be accurate within 0.05 G.

4.3. Biological assays

4.3.1. Binding assays

Membranes from transfected cells with human CB_1 or CB_2 expressed cannabinoid receptors (RBHCB1M400UA and RBXCB2M400UA) were supplied by Perkin-Elmer Life and Analytical Sciences (Boston, MA). The CB_1 receptor membrane proteins concentration was 2.33 pmol/mg or 3.60 pmol/mg depending on the batch and the protein concentration was 8.0 mg/ml. The CB_2 receptor membrane protein concentration was 5.20 pmol/mg or 6.20

pmol/mg and the protein concentration was 4.0 mg/ml or 3.6 mg/ml depending on the batch. The commercial membranes were diluted (approximatively1:20) with the binding buffer (50 mM TrisCl, 5 mM $MgCl_2.H_2O$, 2.5 mM EDTA, 0.5 mg/mL BSA and pH = 7.4 for CB_1 binding; 50 mM TrisCl, 5 mM $MgCl_2.H_2O$, 2.5 mM EGTA, 1 mg/mL BSA and pH = 7.5 for CB_2 binding). The final membrane protein concentration was 0.4 mg/mL of incubation volume and 0.2 mg/mL of incubation volume for the CB_1 and the CB_2 receptor assays, respectively. The radioligand used was [^{3}H]-CP55940 (PerkinElmer) at a concentration of membrane K_D x 0.8 nm, and the final volume was 200 µL for CB_1 binding and was 600 µL for CB_2 binding. 96-Well plates and the tubes necessary for the experiment were previously siliconized with Sigmacote (Sigma).

Membranes were resuspended in the corresponding buffer and were incubated with the radioligand and each compound (10^{-4}-10^{-11} M) for 90 min at 30 ºC. Non-specific binding was determined with 10 µM WIN55212-2 and 100 % binding of the radioligand to the membrane was determined by its incubation with membrane without any compound. Filtration was performed by a Harvester® filtermate (Perkin-Elmer) with Filtermat A GF/C filters pretreated with polyethylenimine 0.05%. After filtering, the filter was washed nine times with binding buffer, dried and a melt-on scintillation sheet (Meltilex™ A, Perkin Elmer) was melted onto it. Then, radioactivity was quantified by a liquid scintillation spectrophotometer (Wallac MicroBeta Trilux, Perkin-Elmer). Competition binding data were analyzed by using GraphPad Prism program and K_i values are expressed as mean ± SD of at least three experiments performed in triplicate for each point.

4.3.2. In vitro antiproliferative assays

Cell culture. The cell lines used in this work were obtained from the American Type Culture Collection (ATCC, Manasas, VA, USA). Prostate LNCaP (ATCC CRL-1740) and

PC-3 cells (ATCC CRL-1435) (Rockville, MD, USA) were routinely growth in RPMI 1640 supplemented with 10% fetal calf serum, 100 U/ml penicillin G, 100 μg/ml streptomycin, and 0.25 μg/ml amphotericin B (Invitrogen, Paisley, UK). Human hepatocellular carcinoma HepG2 cells (ATCC, HB-8065) (Rockville, MD, USA) were growth in DMEM/10%FBS supplemented with 1% non-essential amino acids and 100 IU/mL penicillin G sodium, 100 μg/mL streptomycin sulfate, 0.25 μg/mL amphotericin B (Invitrogen, Paisley, UK). In all cell types, low cell passages (between 10 and 20) were used. One day prior to the experiments medium was changed to 0.5 % FBS medium. Experiments were done when cell monolayers were 80% confluent.

Cell viability assay. Cells in logarithmic phase were cultured at a density of 5000 cells/cm^2 in a 12-well plate. The cells were treated with the medium containing the compounds at concentrations ranging from 0 to 100 μM for 2 days, and finally the MTT reduction assay was carried out as described previously [23], to evaluate the effects of the different compounds on cell growth and to determine the IC_{50}. Briefly, cells were incubated for 1 h at 37ºC with 0,3 mg/ml of 3-[4,5-dimethylthiazolyl-2] 2,5-diphenyl-tetrazolium bromide (MTT) and then were solubilized with 500 μl isopropanol. Absorbance at 570 nm was measured with a plate spectrophotometer (ELX 800 Bio-Tek Instruments, INC).

Flow cytometry. Flow cytometry was used to detect apoptotic cells and the distribution of cell cycle. After being cultivated with medium alone or medium containing the indicated stimuli, 10^5 cells in 35 mm culture dish were harvested in tripsin, fixed in 70% ethanol and stained with 0.05 mg/ml Propidium iodide (PI) plus 0.2 mg/ml RNAse to indicate relative DNA content. The sub-G1 peak (DNA content less than 2 N) and cell cycle distribution were measured with FACScan flow cytometer (Beckton Dickinson, CA, Costa Rica). To analyze apoptosis by Annexin V staining, the cells were washed twice with PBS and incubated in 0.5 ml of Binding Buffer (10 mM HEPES pH 7.4, 150 mM NaCl, 2.5 mM $CaCl_2$, 1 mM $MgCl_2$,

and 4% BSA), with **4** μg/ml Annexin V-FITC for 15 min. Cells were then washed in PBS and resuspended in Binding Buffer with 0.6 μg/ml iodure propidium (IP), (Calbiochem, USA). 20000 cells of each sample were analyzed by flow cytometry in a FACScan (Beckton Dickinson, CA, Costa Rica).

4.3.3. In vivo antitumor assays

Animal care and handling. Athymic nude (nu/nu) (BALB/cOlaHsd-Foxn1^{nu}) five week-old male mice were obtained from Harlan Iberica Laboratory (Barcelona, Spain) and maintained under specific pathogen-free conditions with the approval of the Institutional Ethical Research Committee of Alcala University. All animal studies were conducted in accordance with the Spanish institutional regulation for the housing, care and use of experimental animals and met the European Community directives regulating animal research. Recommendations made by the United Kingdom coordinating Committee on Cancer Research (UKCCCR) have been kept carefully.

In vivo studies. To study the in vivo antitumor activity of **4,** prostate tumors were induced in athymic mice nu/nu (BALB/cOlaHsd-Foxn1^{nu}). Mice were injected subcutaneously in the right flank with 10 x 10^6 LNCaP or PC-3 cells in 0.1 ml of PBS + 0.5% BSA. Two weeks after transplantation, tumors had grown to an average volume of 150 mm^3. Mice were then divided into different experimental groups of 8 animals each, which were treated with 2.0 mg/Kg of compound **4** intraperitoneally injected. The injection was repeated every day and treatment was continued for 15 days. Tumor volumes were monitored every day using calliper measurements and were calculated by the formula: (4π/3)x (w/2)2x (l/2). The body weight of the animals was recorded daily. At the end of the treatment the animals were sacrificed and xenografted tumors were weighted and frozen.

4.4. In silico calculations of ADME properties

A set of 34 physicochemical descriptors was computed using QikProp version 3.5 integrated in Maestro (Schrödinger, LLC, New York, USA). The 3D conformations used in the calculation of QikProp descriptors were generated using the program Spartan ´08 (Wave function, Inc., Irvine CA) as follows: the structure of each molecule was built from the fragment library available in the program. Then, *ab initio* energy minimizations of each structure at the Hartree-Fock 6-31G* level were performed. A conformational search was next implemented using Molecular Mechanics (Monte Carlo method) followed by a minimization of the energy of each conformer calculated at the Hartree-Fock 6-31G* level. The global minimum energy conformer of each compound was used as input for ADME studies with QikProp.

Acknowledgements

Financial support by Spanish Grants from Spanish Ministry of Economy and Competitivity SAF2012-40075-C02-02, SAF2009-12422-C02-02, SAF2008-03220, BFU2012-31444, Comunidad de Madrid CAM S2010/BMD-2308 and Alcalá University GC2011-001 is gratefully acknowledged. P.M. is recipient of a fellowship JAE-Pre-2010-01119 from Junta para la Ampliación de Estudios co-financed by FSE.

Appendix. Supplementary material

Supplementary data associated with this article can be found, in the online version, at

References

[1] L. G. Gomella, X. L. S. Liu, E. J. Trabulsi, W. K. Kelly, R. Myers, T. Showalter, A. Dicker, R. Wender, Screening for prostate cancer: the current evidence and guidelines controversy, Can. J. Urol. 18 (2011) 5875–5883.

[2] W. H. Fu, E. Madan, M. Yee, H. T Zhang, Progress of molecular targeted therapies for prostate cancers, BBA-Rev. Cancer 1825 (2012) 140–152.

[3] N. M. O'Boyle, M. J. Meegan, Designed multiple ligands for cancer therapy, Cur. Med. Chem. 18 (2011) 4722–4737.

[4] L. K. Gediya, V. C. O. Njar, Promise and challenges in drug discovery and development of hybrid anticancer drugs, Expert Opin. Drug Dis. 4 (2009) 1099–1111.

[5] R. G. Pertwee, Emerging strategies for exploiting cannabinoid receptor agonists as medicines, Br. J. Pharmacol. 156 (2009) 397–411.

[6] G. Velasco, C. Sanchez, M. Guzman, Towards the use of cannabinoids as antitumour agents, Nat. Rev. Cancer 12 (2012) 436–444.

[7] M. Guzman, Cannabinoids: potential anticancer agents, Nat. Rev. Cancer 3 (2003) 745–755.

[8] S. Sarfaraz, V. M. Adhami, D. N. Syed, F. Afaq, H. Mukhtar, Cannabinoids for cancer treatment: progress and promise, Cancer Res. 68 (2008) 339–342.

[9] D. H. P. de la Ossa, M. Lorente, M. E. Gil-Alegre, S. Torres, E. Garcia-Taboada, M. D. Aberturas, J. Molpeceres, G. Velasco, A. I. Torres-Suarez, Local delivery of cannabinoid-loaded microparticles inhibits tumor growth in a murine xenograft model of glioblastoma multiforme, PLoS One 8 (2013) e54795.

[10] C. Grimaldi, A. Capasso, The endocannabinoid system in the cancer therapy: An overview, Curr. Med. Chem. 18 (2011) 1575–1583.

[11] C. J. Fowler, S. B. Gustafsson, S. C. Chung, E. Persson, S. O. P. Jacobsson, A. Bergh, Targeting the endocannabinoid system for the treatment of cancer - A practical view, Curr. Top. Med. Chem. 10 (2010) 814–827.

[12] C. Manera, G. Saccomanni, A. M. Malfitano, S. Bertini, F. Castelli, C. Laezza, A. Ligresti, V. Lucchesi, T. Tuccinardi, F. Rizzolio, M. Bifulco, V. Di Marzo, A. Giordano, M. Macchia, A. Martinelli, Rational design, synthesis and anti-proliferative properties of new CB2 selective cannabinoid receptor ligands: An investigation of the 1,8-naphthyridin-2(1H)-one scaffold, Eur. J. Med. Chem. 52 (2012) 284–294.

[13] A. M. Malfitano, E. Ciaglia, G. Gangemi, P. Gazzerro, C. Laezza, M. Bifulco, Update on the endocannabinoid system as an anticancer target, Expert Opin. Ther. Tar. 15 (2011) 297–308.

[14] I. Diaz-Laviada, The endocannabinoid system in prostate cancer, Nat. Rev. Urol. 8 (2011) 553–561.

[15] K. Nithipatikom, M. A. Isbell, M. P. Endsley, J. E. Woodliff, W. B. Campbell, Anti-proliferative effect of a putative endocannabinoid, 2-arachidonylglyceryl ether in prostate carcinoma cells, Prostag. Oth. Lipid M. 94 (2011) 34–43.

[16] I. Brown, M. G. Cascio, K. W. J. Wahle, R. Smoum, R. Mechoulam, R. A. Ross, R. G. Pertwee, S. D. Heys, Cannabinoid receptor-dependent and -independent anti-proliferative effects of omega-3 ethanolamides in androgen receptor-positive and -negative prostate cancer cell lines, Carcinogenesis 31 (2010) 1584–1591.

[17] C. Asche, Antitumour quinones, Mini Rev. Med. Chem. 5 (2005) 449-467.

[18] N. M. Kogan, R. Rabinowitz, P. Levi, D. Gibson, P. Sandor, M. Schlesinger, R. Mechoulam, Synthesis and antitumor activity of quinonoid derivatives of cannabinoids, J. Med. Chem. 47 (2004) 3800–3806.

[19] N. M. Kogan, M. Schlesinger, M. Peters, G. Marincheva, R. Beeri, R. A. Mechoulam, Cannabinoid anticancer quinone, HU-331, is more potent and less cardiotoxic than doxorubicin: a comparative in vivo study, J. Pharmacol. Exp. Ther. 322 (2007) 646–653.

[20] J. Cumella, L. Hernandez-Folgado, R. Giron, E. Sanchez, P. Morales, D. P. Hurst, M. Gomez-Canas, M. Gomez-Ruiz, D. C. Pinto, P. Goya, P. H. Reggio, M. I. Martin, J. Fernandez-Ruiz, A. M. Silva, N. Jagerovic, Chromenopyrazoles: non-psychoactive and selective CB(1) cannabinoid agonists with peripheral antinociceptive properties, ChemMedChem 7 (2012) 452–446.

[21] S. Akai, Y. Kita, Recent progress in the synthesis of p-quinones and p-dihydro-quinones through oxidation of phenol derivative. A review, Org. Prep. Proced. Int. 30 (1998) 603–629.

[22] R. Barret, M. Daudon, Oxidation of phenols to quinones by bis(trifluoroacetoxy)iodobenzene, Tetrahedron Lett. 31 (1990) 4871–4872.

[23] S. Malagarie-Cazenave, N. Olea-Herrero, D. Vara, I. Diaz-Laviada, Capsaicin, a component of red peppers, induces expression of androgen receptor via PI3K and MAPK pathways in prostate LNCaP cells, FEBS Lett. 583 (2009) 141–147.

[24] S. Sarfaraz, F. Afaq, V. M. Adhami, H. Mukhtar, Cannabinoid receptor as a novel target for the treatment of prostate cancer, Cancer Res. 65 (2005) 1635–1641.

[25] O. M. Darwish, G. V. Raj, Management of biochemical recurrence after primary localized therapy for prostate cancer, Front. Oncol. 2 (2012) 48.

[26] M. Grossmann, J. D. Zajac, Androgen deprivation therapy in men with prostate cancer: how should the side effects be monitored and treated?, Clin. Endocrinol. 74 (2011) 289–293.

[27] M. C. Kim, H. C. Kwon, S. N. Kim, H. S. Kim, B. H. Um, Plastoquinones from Sargassum yezoense; chemical structures and effects on the activation of peroxisome proliferator-activated receptor gamma, Chem. Pharm. Bull. 59 (2011) 834-838.

[28] J. Xue, W. Ding, Y. Liu, Anti-diabetic effects of emodin involved in the activation of PPARgamma on high-fat diet-fed and low dose of streptozotocin-induced diabetic mice, Fitoterapia 81 (2010) 173-177.

[29] C. C. Woo, S. Y. Loo, V. Gee, C. W. Yap, G. Sethi, A. P. Kumar, K. H. Tan, Anticancer activity of thymoquinone in breast cancer cells: possible involvement of PPAR-gamma pathway, Biochem. Pharmacol. 82 (2011) 464-475.

[30] C. C. Yu, P. J. Wu, J. L. Hsu, Y. F. Ho, L. C. Hsu, Y. J. Chang, H. S. Chang, I. S. Chen, J. H. Guh, Ardisianone, a natural benzoquinone, efficiently induces apoptosis in human hormone-refractory prostate cancers through mitochondrial damage stress and survivin downregulation, Prostate 73 (2013) 133-145.

[31] C. C. Lee, K. F. Huang, P. Y. Lin, F. C. Huang, C. L. Chen, T. C. Chen, J. H. Guh, J. J. Lin, H. S. Huang, Synthesis, antiproliferative activities and telomerase inhibition evaluation of novel asymmetrical 1,2-disubstituted amidoanthraquinone derivatives, Eur. J. Med. Chem. 47 (2012) 323-336.

[32] G. Z. Jin, H. S. Jin, L. L. Jin, Synthesis and antiproliferative activity of 1,4-bis(dimethylamino)-9,10-anthraquinone derivatives against P388 mouse leukemic tumor cells, Arch. Pharm. Res. 34 (2011) 1071-1076.

[33] Y. Kumagai, Y. Shinkai, T. Miura, A. K. Cho, The chemical biology of naphthoquinones and its environmental implications, Annu. Rev. Pharmacol. 52 (2012) 221-247.

Figure captions

Figure 1. Quinone structures related to cannabinoids.

Figure 2. Cyclic voltammotric curves of 1 mM **4** sweep rates ranging from 0.1 to 2 V/s in 100% DMSO with 0.1M TBAP.

Figure 3. ESR experimental and simulated spectrum of **4** in DMSO.

Figure 4. Chromenopyrazolediones **4-6** decrease human cancer cell viability. Human hepatocellular carcinoma HepG2 and human prostate cancer LNCaP and PC-3 cells were incubated for 48 h with increasing doses of the tested compounds. Cell viability was determined by MTT. Data are the mean ± S.D. of two different experiments performed in triplicate.

Figure 5. Chromenopyrazoledione **4** induces cell cycle arrest in human prostate cancer cells. Cell cycle analysis of human prostate LNCaP and PC-3 cells treated with the IC_{50} (15 µM) of **4** for 24 h. Cells were stained with IP and analyzed by flow cytometry. Figure is representative of other two performed in duplicate.

Figure 6. Chromenopyrazoledione **4** induces apoptosis in human prostate cancer cells. Evaluation of apoptosis by annexin V-FITC/PI staining followed by flow cytometric analysis. Representative plots of annexin V-FITC/PI staining of LNCaP or PC-3 cells cultured in the presence of the IC_{50} (15 µM) of **4** for 24 h are shown. Data showing the percentage of late apoptotic cells (upper right quadrant) are the mean ± S.D. of three different experiments performed in duplicate.

Figure 7. Signalling pathways involved in antiproliferative effect produced by compound **4**. LNCaP cells were incubated for 48 h with vehicle (control) or with **4** at IC_{50} dose (20 µM) in

presence or not of different inhibitors (CB_1 antagonist, SR1; CB_2 antagonist, SR2; PPARγ antagonist, GW9662; and the antioxidant N-acetylcysteine, NAC). Cell viability was determined by MTT. Results represent the mean ± S.E. of four different experiments performed in duplicate. * $p \leq 0,05$ compared with Student's test versus NAC treated cells and # $p \leq 0,05$ compared with Student's test versus the compound alone.

Figure 8. In vivo antitumoral effect of compound **4**. Athymic nude mice were injected s.c. in the right flank with either LNCaP (A) or PC-3 (B) cells and four weeks later (day 0) treated during 15 days with vehicle (control) or 2 mg/kg of **4**. Treatments were administered intraperitoneally every day. Tumor growth curves are represented in the graph. Results represent the mean ± S.E. of eight mice in each group. A representative dissected tumor after the treatment is shown on the right.

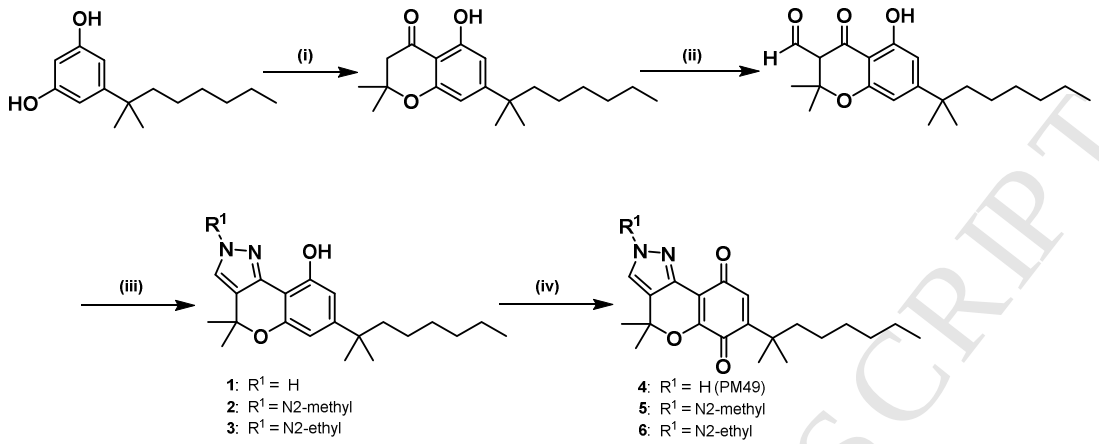

[a] Reaction conditions: (i) 3,3-dimethylacrylic acid, CH_3SO_3H, P_2O_5, 70°C, MW, 10 min; (ii) NaH, THF, MW, 46°C, 20 min then ethyl formate, THF, MW, 46 °C, 20 min; (iii) H_2N-NHR_2, EtOH, 16h, room temperature; (iv) [bis(trifluoro-acetoxy)iodo]benzene, MeCN/ H_2O (6:1), 15 min, room temperature.

Scheme 1. Oxidation of chromenopyrazoles to the corresponding quinone derivatives **4**-**6.**[a]

Table 1. Binding affinity of quinoid derivatives of chromenopyrazoles **4**-**6** and the reference cannabinoid WIN55,212-2 for *h*CB_1 and *h*CB_2 cannabinoid receptors.

Compd	*h*CB_1 K_i (nM)[a]	*h*CB_2 K_i (nM) [a]
4	324±235	134±21
5	14180±5638	672±191
6	8520±3891	3665±878
WIN55,212-2	45.6±8.6	3.7±0.2

[a]Values obtained from competition curves using [^{3}H]CP55940 as radioligand for *h*CB_1 and *h*CB_2 cannabinoid receptors and are expressed as the mean ± SEM of at least three experiments.

Properties	Calculated	Range 95 % of drugs
Aqueous solubility (QPlogS)	-5.157	-6.5/0.5
Blood brain barrier penetration (QlogBB)	-1.015	-3.0/1.2
HERG K+ channel blockage (logIC50)	-4.698	Concern below -5
Apparent Caco-2 permeability (nm/s)	666	<25% is poor; >500 is excellent
% Human oral absorption gastrointestinal	100	<25% is poor

Table 2. Predicted ADME parameters *in silico* calculated for compound **4.**

Figure 1

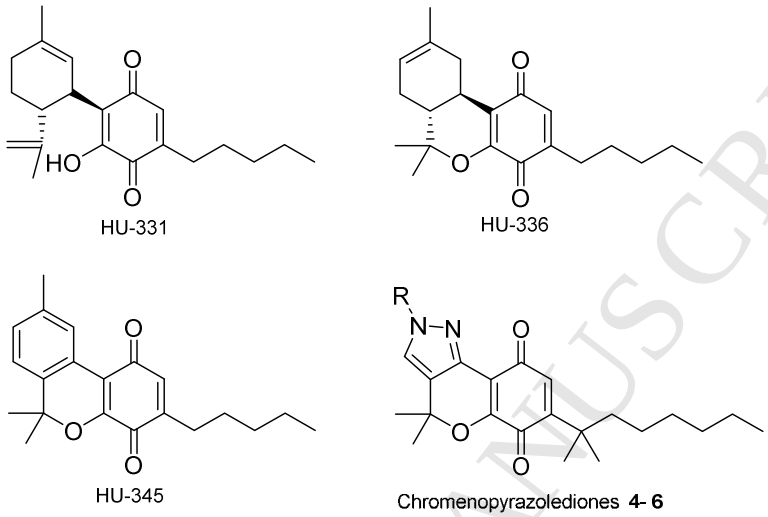

Figure 2

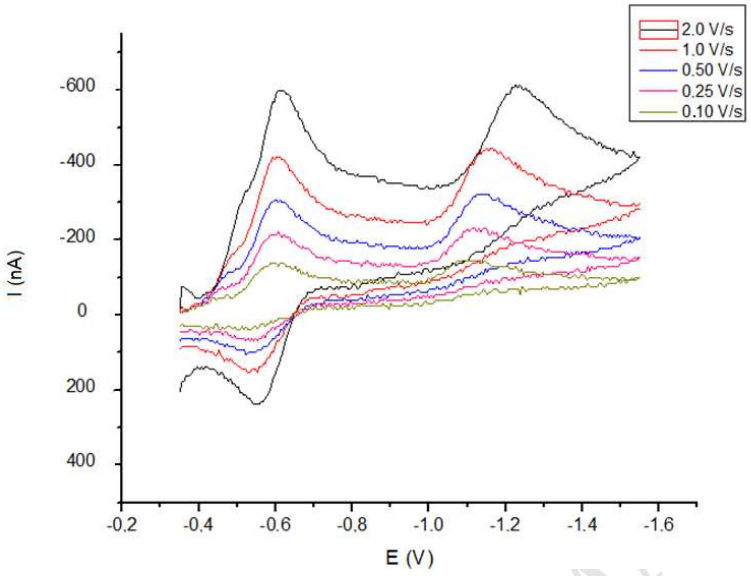

Figure 3

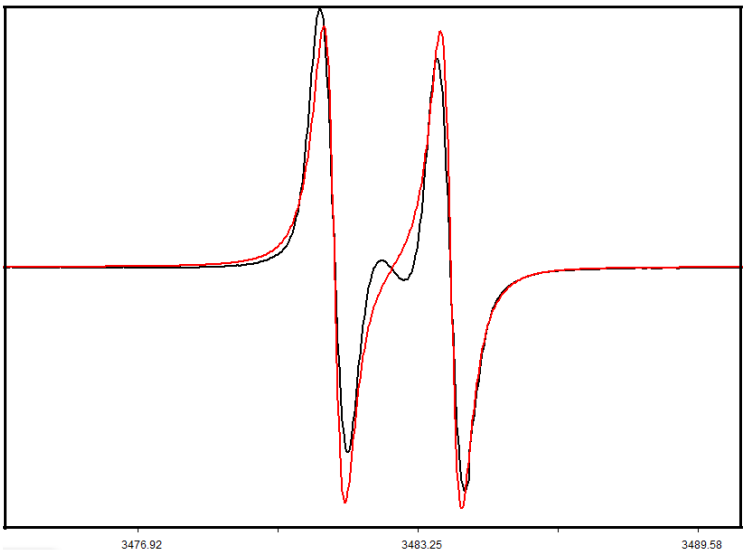

Figure 4

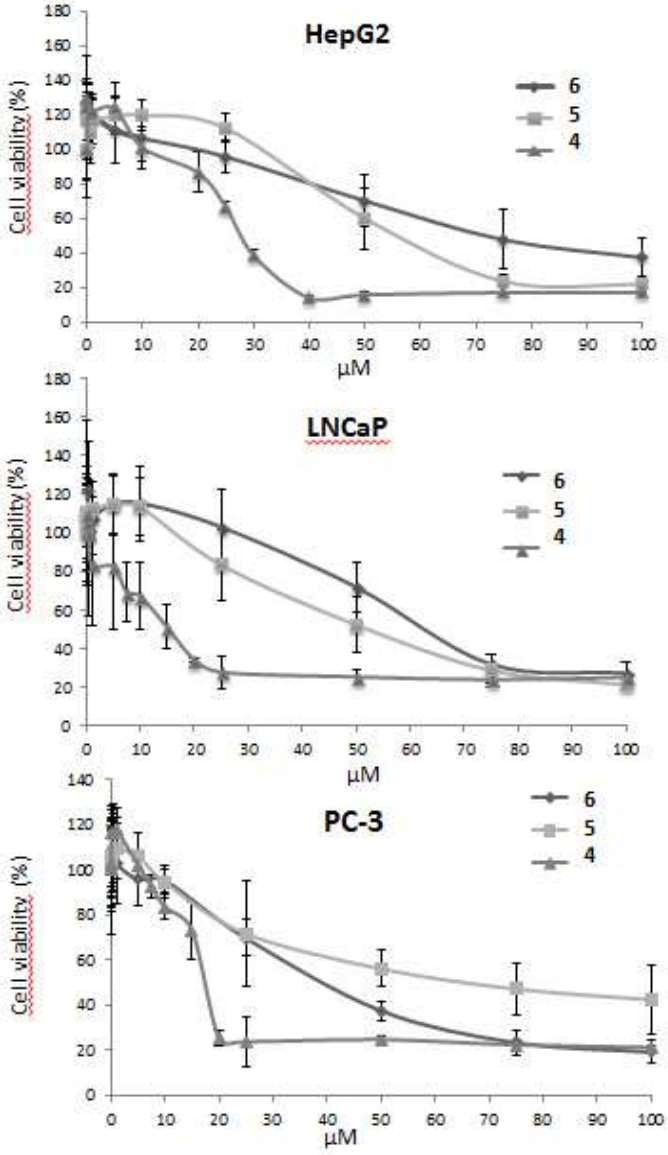
HepG2
Cell viability (%)
µM
6
5
4
LNCaP
Cell viability (%)
µM
6
5
4
PC-3
Cell viability (%)
µM
6
5
4

Figure 5

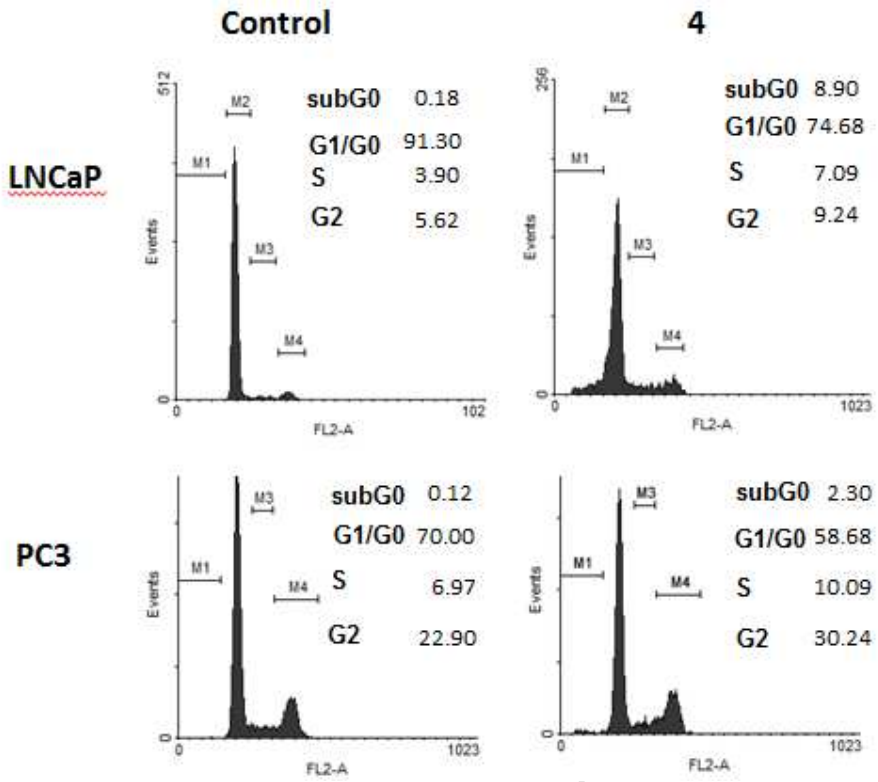

Figure 6

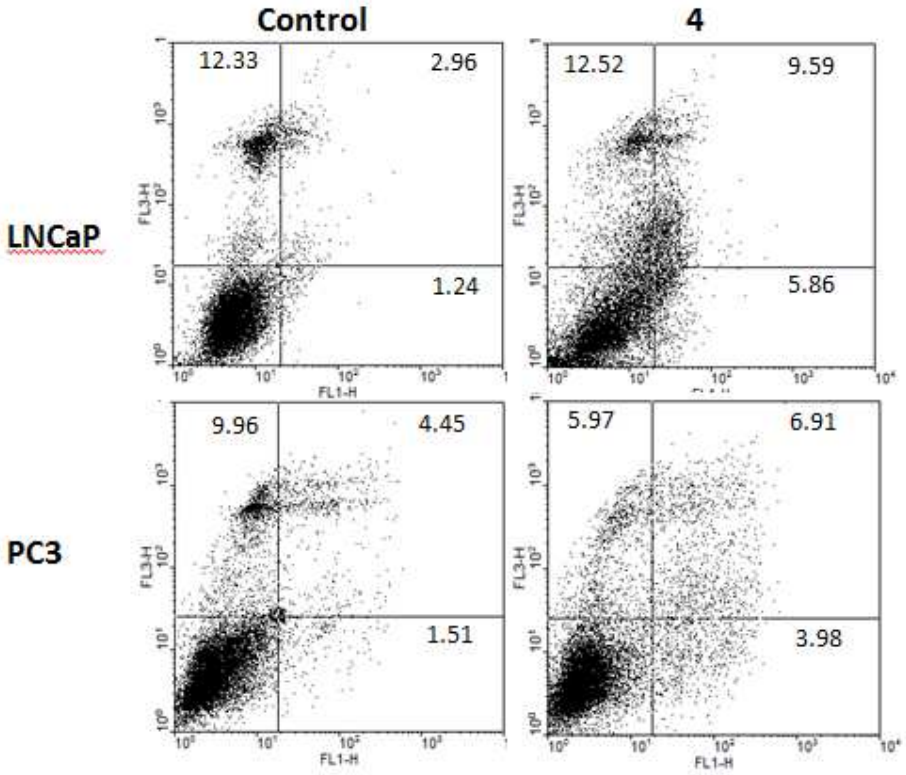

Figure 7

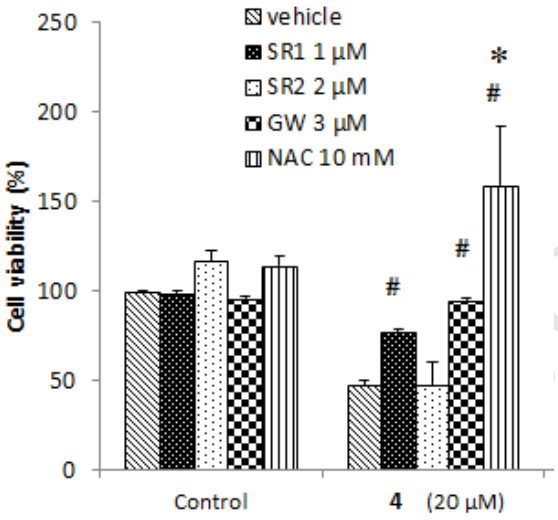

Figure 8

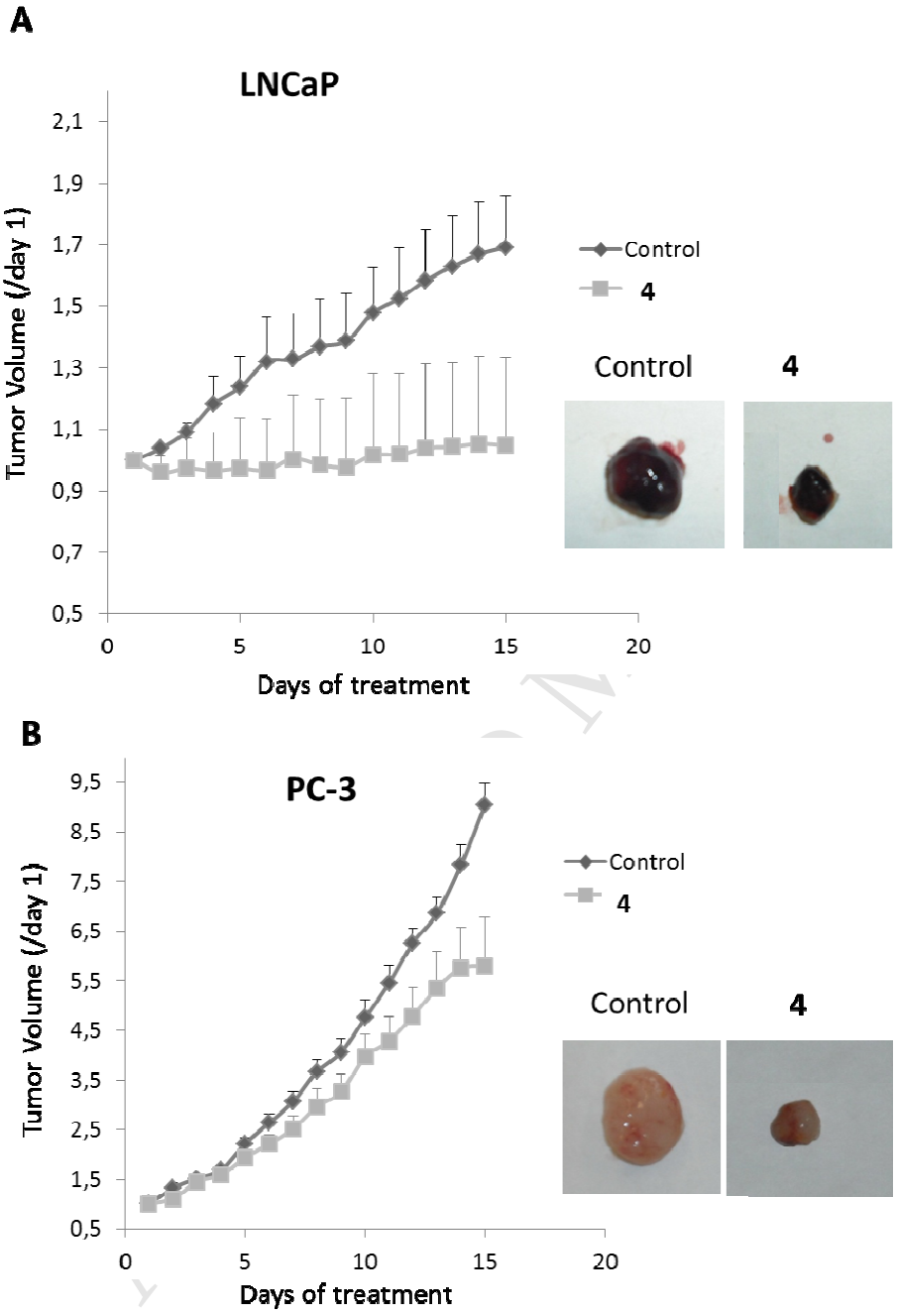
A
LNCaP
Tumor Volume (/day 1)
2,1
1,9
1,7
1,5
1,3
1,1
0,9
0,7
0,5
0
5
10
15
20
Days of treatment
Control
4
Control
4
B
PC-3
Tumor Volume (/day 1)
9,5
8,5
7,5
6,5
5,5
4,5
3,5
2,5
1,5
0,5
0
5
10
15
20
Days of treatment
Control
4
Control
4

Supplementary Material

Synthetic cannabinoid quinones: preparation, in vitro antiproliferative Effects and in vivo prostate antitumor activity

Paula Morales[a], Diana Vara[b], María Goméz-Cañas[c], María C. Zúñiga[d], Claudio Olea-Azar[d], Pilar Goya[a], Javier Fernández-Ruiz[c], Inés Díaz-Laviada[b]*, Nadine Jagerovic[a]*

[a]*Instituto de Química Médica, CSIC, Calle Juan de la Cierva, 3, 28006 Madrid, Spain*
[b]*Departamento de Bioquímica y Biología Molecular, Facultad de Medicina, Universidad de Alcalá, Alcalá de Henares, 28871 Madrid, Spain*
[c]*Departamento de Bioquímica y Biología Molecular, Facultad de Medicina, Centro de Investigación Biomédica en Red sobre Enfermedades Neurodegenerativas (CIBERNED), Instituto Ramón y Cajal de Investigación Sanitaria (IRYCIS), Universidad Complutense de Madrid, 28040 Madrid, Spain*
[d]*Departamento de Química Inorgánica y Analítica, Facultad de Ciencias Químicas y Farmacéuticas, Universidad de Chile, Casilla 233, Santiago 1, Chile*

Contents:

- **Table 1**. Cyclic voltammetric parameters of **4** and **6** *vs.* saturated calomel electrode at 2.0 V/s

Compd	$E_{pc\ I}$ (mV)	$E_{pa\ I}$ (mV)	$E_{1/2}$ (mV)	I_{pa}/I_{pc}	$E_{pc\ II}$ (mV)
4	-0.512	-0.422	-0.467	0.54	-1.263
6	-0.590	-0.527	-0.559	0.65	-1.141

- **Analytical data: elemental analysis of 4, 5 and 6.**

Compound **4**. Anal.: $C_{21}H_{28}N_2O_3$ (356,46 g/mol) Calculated: C, 70.76%; H, 7.92%. Experimental: C, 71.03%; H, 8.24%.

Compound **5**. Anal.: $C_{22}H_{30}N_2O_3$ (370,49 g/mol) Calculated: C, 71.32%; H, 8.16%. Experimental: C, 70.98%; H, 8.31%.

Compound **6**. Anal.: $C_{23}H_{32}N_2O_3$ (384,51 g/mol) Calculated: C, 71.84%; H, 8.39%. Experimental: C, 72.01%; H, 8.62%.

- ^{1}H- and ^{13}C-NMR spectra of 4, 5 and 6 in $CDCl_3$.

Fig. S1. ^{1}H-NMR ($CDCl_3$, 300 MHz): 7-(1',1'-Dimethylheptyl)-1,4-dihydro-4,4-dimethylchromeno[4,3-c]pyrazol-6,9-dione (**4**)

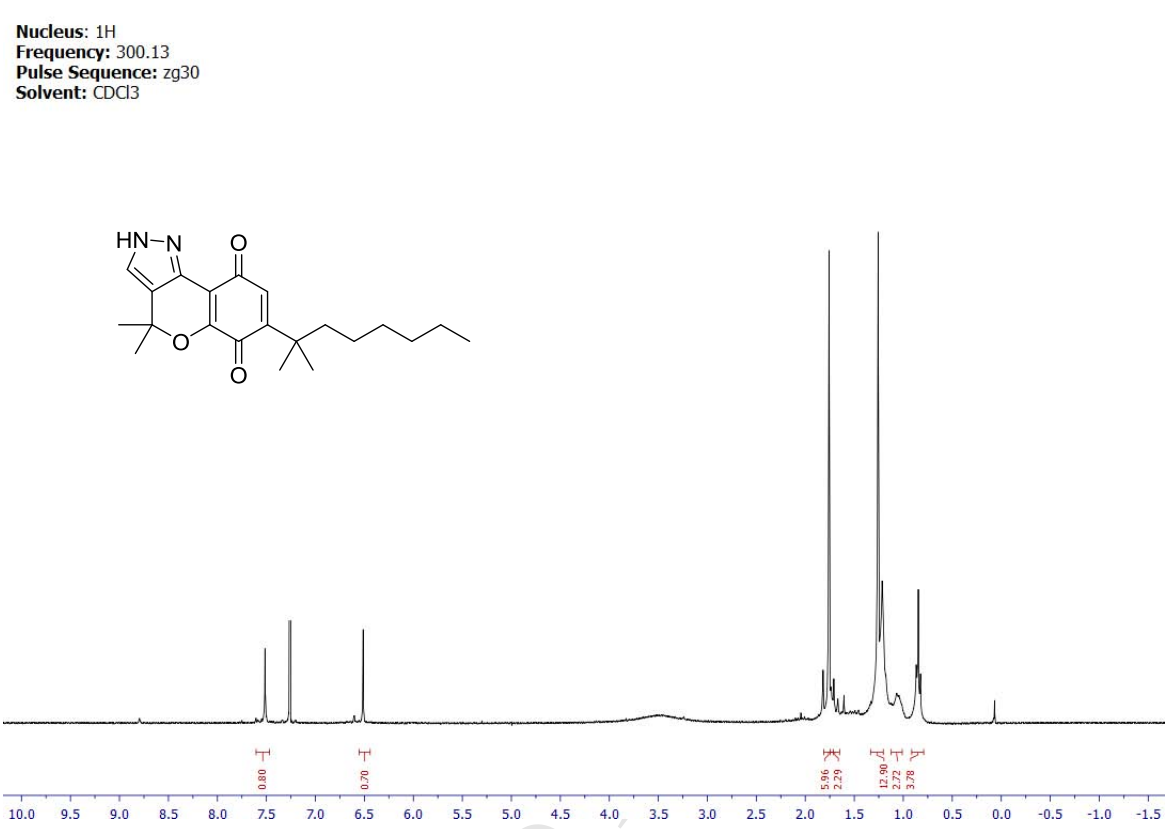

Fig. S2. ^{13}C-NMR ($CDCl_3$, 75 MHz): 7-(1',1'-Dimethylheptyl)-1,4-dihydro-4,4-dimethylchromeno[4,3-*c*]pyrazol-6,9-dione (**4**)

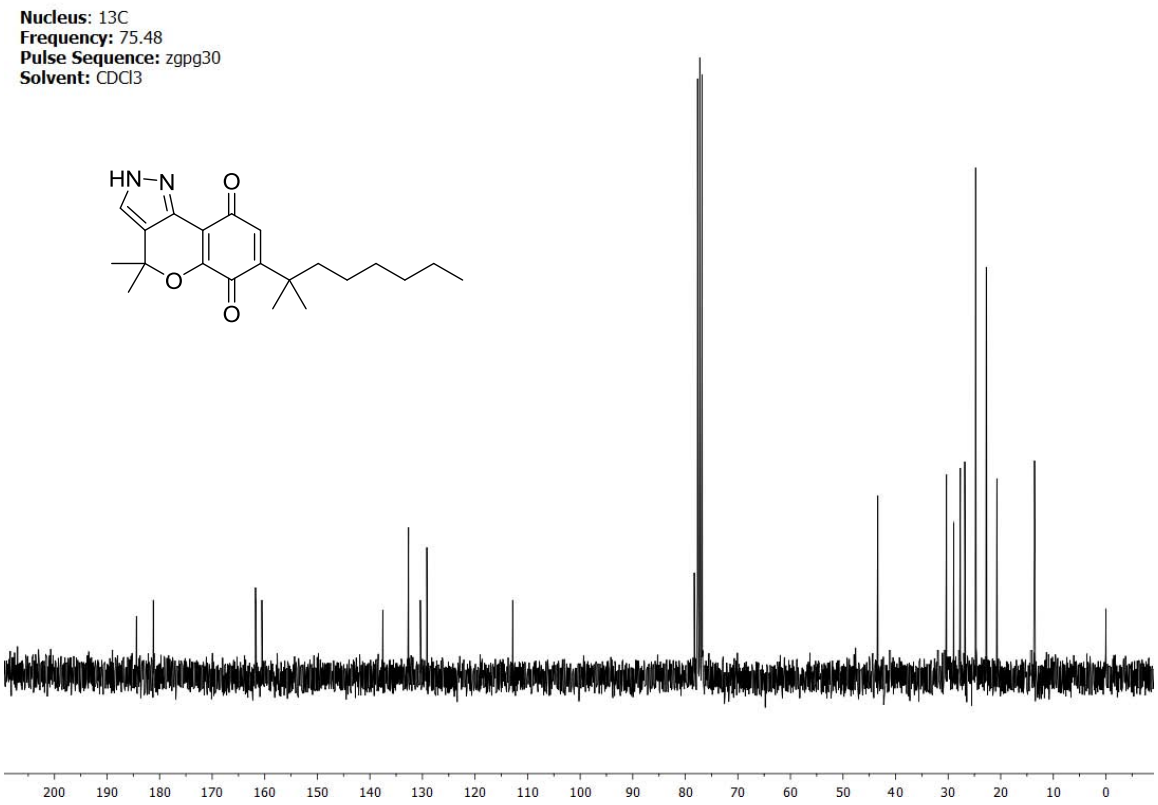

Fig. S3. ^{1}H-NMR ($CDCl_3$, 300 MHz): 7-(1',1'-Dimethylheptyl)-2,4-dihydro-2,4,4-trimethylchromeno[4,3-c]pyrazol-6,9-dione (**5**)

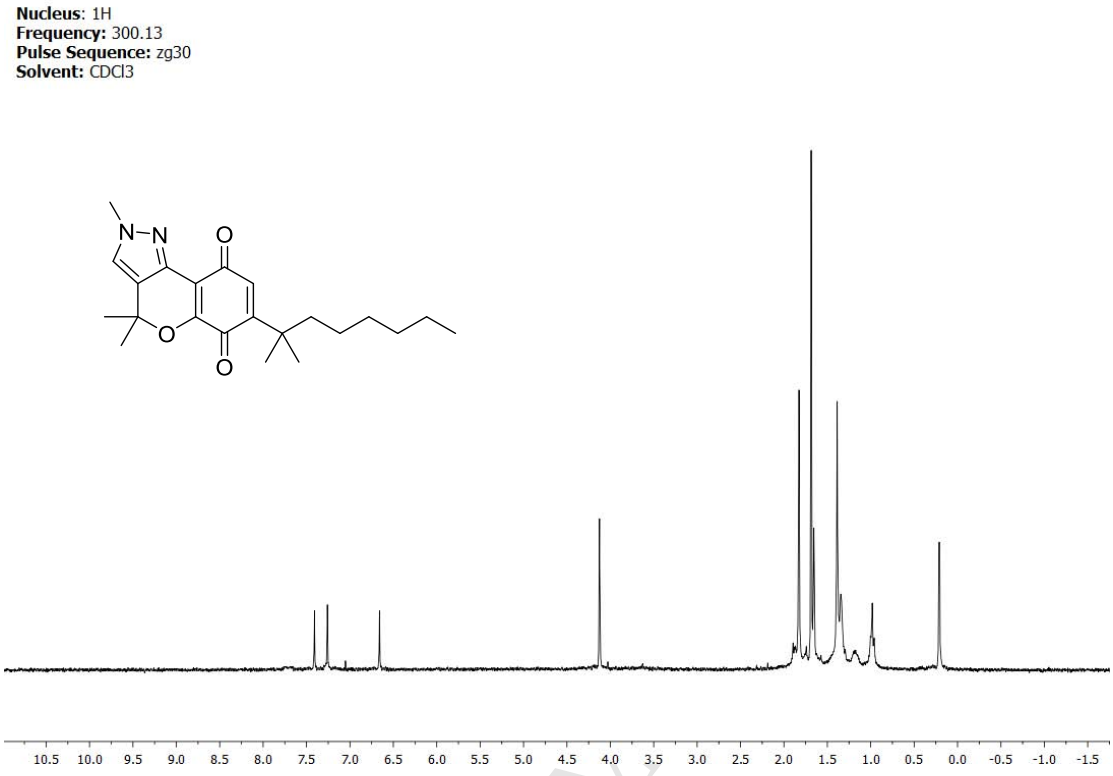

Fig. S4. ^{13}C-NMR ($CDCl_3$, 75 MHz): 7-(1',1'-Dimethylheptyl)-2,4-dihydro-2,4,4-trimethylchromeno[4,3-c]pyrazol-6,9-dione (**5**)

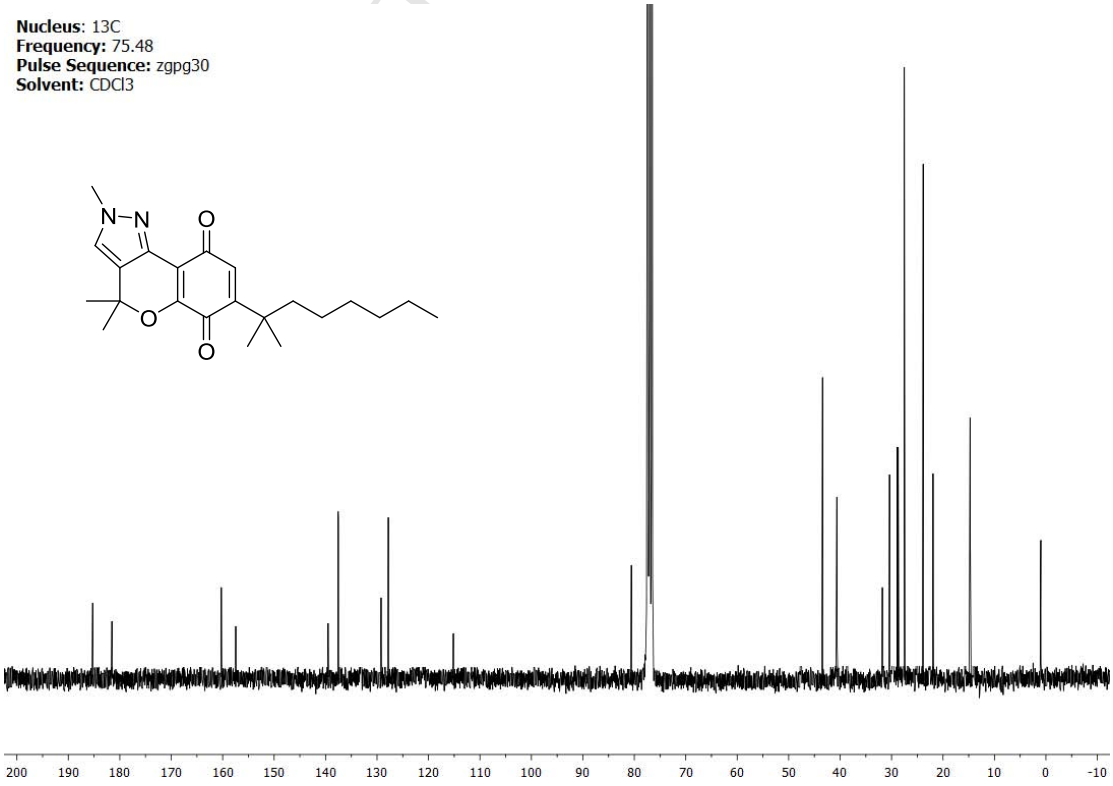

Fig. S5. ^{1}H-NMR ($CDCl_3$, 300 MHz): 7-(1',1'-Dimethylheptyl)-2-ethyl-2,4-dihydro-4,4-dimethylchromeno[4,3-c]pyrazol-6,9-dione (**6**)

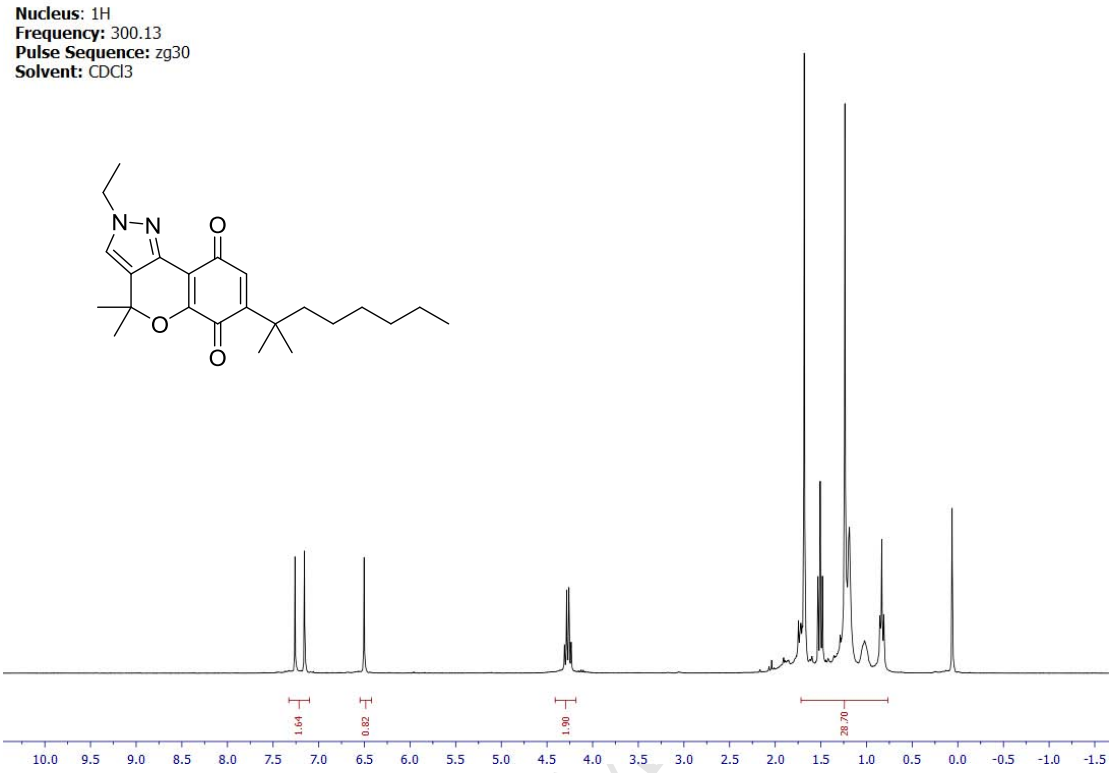

Fig. S6. ^{13}C-NMR ($CDCl_3$, 75 MHz): 7-(1',1'-Dimethylheptyl)-2-ethyl-2,4-dihydro-4,4-dimethylchromeno[4,3-c]pyrazol-6,9-dione (**6**)